

The characterization of boron-doped carbon nanotube arrays

C.F. Chen, C.L. Tsai*, C.L. Lin

Department of Materials Science and Engineering, National Chiao Tung University, 1001 Ta Hsueh Road, Hsinchu 30050, Taiwan, ROC

Received 25 April 2003; received in revised form 25 April 2003; accepted 8 May 2003

Abstract

In this study, we directly synthesized boron-doped carbon nanotubes (CNTs) by using trimethylborate ($B(OCH_3)_3$) as doping sources in a microwave plasma chemical vapor deposition system (MPCVD). Doping boron causes the growth rate of CNTs to decrease. This might be due to the high oxygen content contained in the doping source that induces oxidation of graphite. The bamboo-like nanostructure of the carbon tubes disappeared with boron doping. Raman spectrum shows the higher I_D/I_G ratio in boron-doped CNTs. This implies the decrease of graphitization in boron-doped CNTs. In addition, doping boron could enhance the field emission property by increasing the current density by more than 30% (from 350 to 470 mA/cm² at 2.2 V/ μ m).

© 2003 Elsevier Science B.V. All rights reserved.

Keywords: Nanotubes; p-Type doping; Chemical vapor deposition; Field emission

1. Introduction

Since their first discovery in 1991 [1], carbon nanotubes (CNTs), have been considered for various applications. Their small dimension, high strength and the remarkable physical properties (like high Young's modulus and high-aspect ratio) of these structures make them very promising emitters for field emission devices. Due to the size-effect and structure diversity of nanomaterials, the physical properties strongly depend on their micro structure, size and chemical bonding [2]. Different diameter, length and chirality of CNTs gives rise to diverse physical and mechanical properties. In general, for a semiconductor field emitter, the emitting electrons can originate from the conduction band, the valence band and/or surface states. It is believed that the inclusions such as nitrogen, phosphorus or boron can enhance CNTs' electron properties by offering electrons or holes.

Boron-doped CNTs are predicted to act as semiconductors among large range diameters and chiralities. Boron-doped CNTs (B/C ratio < 0.05) were reported as by-products when BC_2N CNTs were prepared by an arc-discharge method [3]. Recently, we have successfully

synthesized boron-doped diamond-like emitters in microwave plasma chemical vapor deposition (MPCVD) [4]. In this article, selective area deposition (SAD) of boron-doped CNTs was directly completed in MPCVD.

2. Experiment

The starting substrates were mirror-polish n-type, (100) oriented Si wafer with a resistivity of 4.5~5.5 Ω /cm. Wafers were cleaned by Radio Corporation of America (RCA) cleaning process to remove contamination on the silicon surface. After cleaning, a SiO_2 dielectric layer was deposited using high-temperature and low-pressure furnace deposition system (model

Table 1
Deposition conditions

Sample	Flow rate CH_4/H_2 + doping source (sccm)
A (undoped)	10/40
B (boron-doped)	10/40+0.5
C (boron-doped)	10/40+1
D (boron-doped)	10/40+2

Note: Deposition time = 10 min; Total pressure = 15 torr; MW power = 400 W; Substrate temp. ($^{\circ}C$) = \sim 700; Doping source: $B(OCH_3)_3$.

*Corresponding author. Tel.: +886-935889532; fax: +886-62616193.

E-mail address: lun@ms15.url.com.tw (C.L. Tsai).

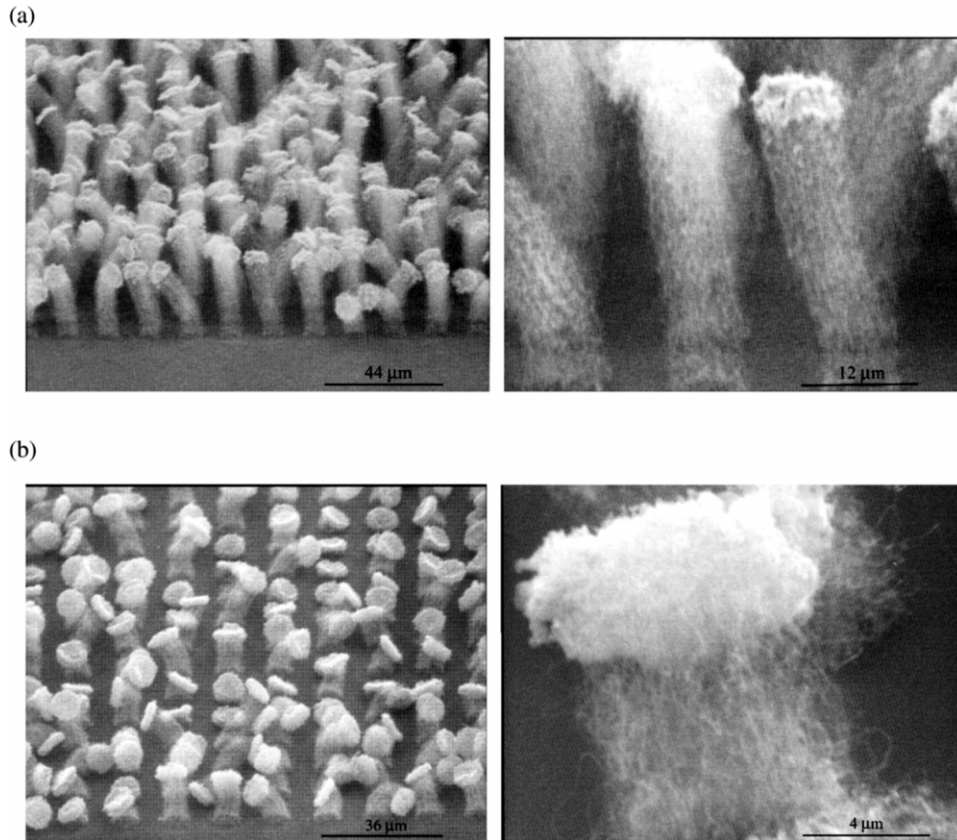


Fig. 1. SEM photographs of (a) undoped and (b) boron-doped CNTs array.

ASM LB-45). A pattern of 8 μm wide dots with 8 μm space between them was successfully fabricated onto a photoresist layer using ASM PAS 2500/10 G-Line exposurer and the Convac CPP-70 developing system. A 150-nm-thick film of Fe catalyst was deposited on

SiO₂ by using dual E-Gun evaporator (model ULVAC EBX-10C, Japan). Then, the photoresist was removed by lift-off process in an acetone solution in an ultrasonic agitator. Finally, the patterned substrates were put in a microwave plasma chemical vapor deposition

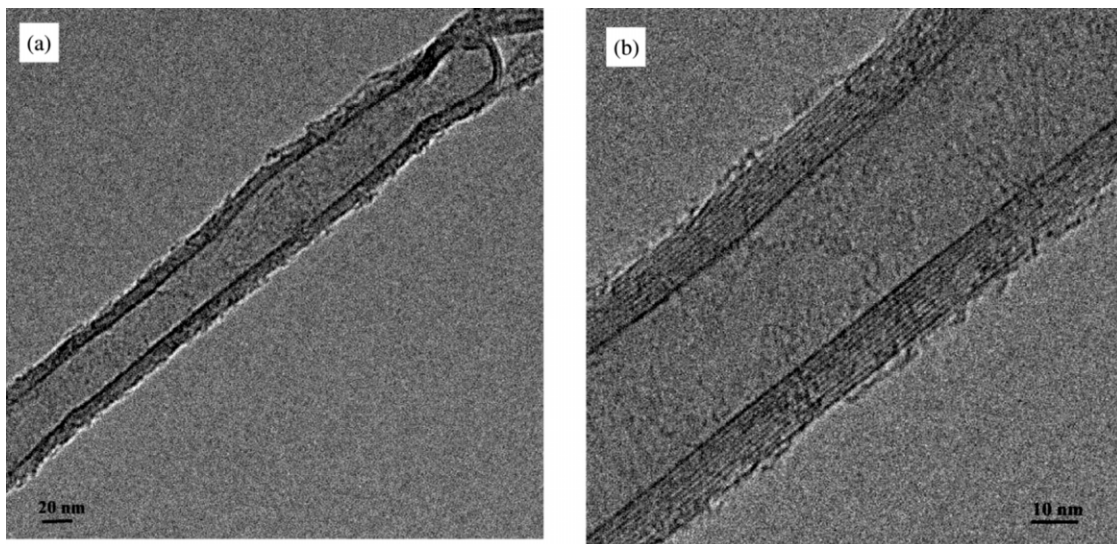


Fig. 2. TEM images of undoped CNTs.

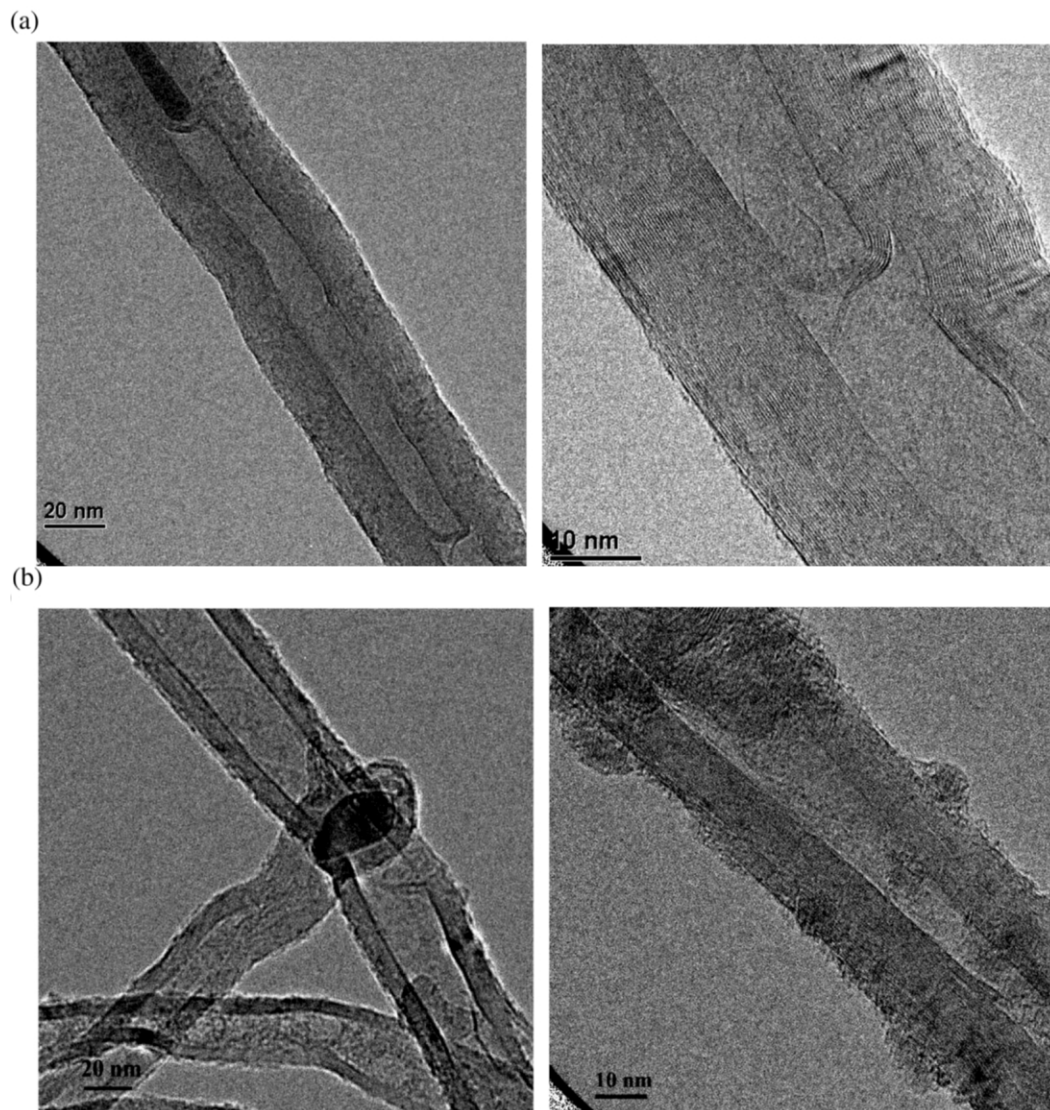


Fig. 3. TEM images of (a) sample C and (b) sample D.

(MPCVD) chamber to grow selective patterned deposition (SAD) of CNTs. The reactive gases used in deposition were $\text{CH}_4\text{-H}_2$ with flow rate of 10/40 sccm and trimethylborate $\text{B}(\text{OCH}_3)_3$ as doping source with 0.5; 1 and 2 sccm, respectively. The average deposition time and substrate temperature were 10 min and 700 °C measured by pyrometer. Table 1 lists the experimental conditions.

The length and the morphology of the produced CNTs were characterized by scanning electron microscopy (SEM). A transmission electron microscopy (TEM) was used to determine the nanostructure of individual CNT. The TEM specimens were prepared by dispersing the CNTs in an acetone ultrasonic bath. A drop of the suspension was placed onto a carbon lace film Cu grid. Raman spectroscopy was used to evaluate the crystallinity. Secondary ion mass spectrometry (SIMS) was used

to detect the amount of boron. An $I\text{-}V$ measuring system was used to obtain the field emission property.

3. Results and discussion

3.1. Scanning electron microscopy (SEM)

Fig. 1a and b show the SEM pictures of undoped and boron-doped CNTs, respectively. The photograph on the right side of each figure is an enlarged image. Eight micrometer-bound aligned CNTs are successfully completed through selective area deposition method. Obviously, it is found that the undoped CNTs are longer length. Under the SEM analysis, we find that undoped CNTs are denser than boron-doped ones. This could be explained by the high oxygen content contained in the $\text{B}(\text{OCH}_3)_3$. High concentration of oxygen increases the

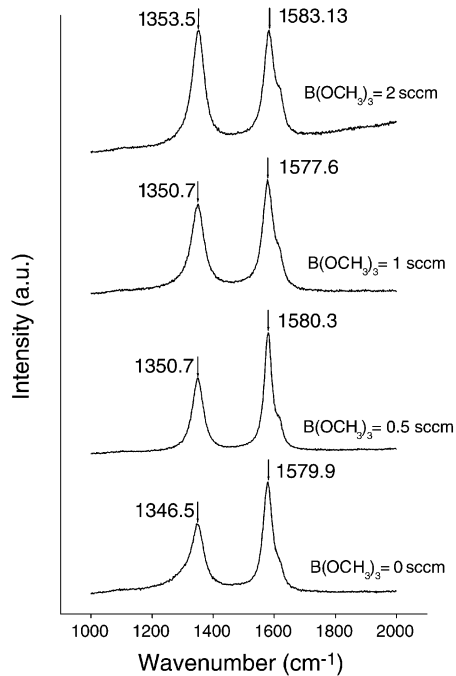


Fig. 4. Raman spectrum of undoped and various concentrations of boron-doped CNTs.

etching rate during CNTs growth under 700 °C. This is in accordance with our previous study, where the growth of diamond was inhibited when O₂ was added to the CH₄-CO₂ gas mixture [5].

3.2. Transmission electron microscopy (TEM)

Figs. 2 and 3 show the TEM images of undoped and boron-doped CNTs, respectively. In Fig. 3, the right side pictures are enlarged images of the ones on the left. Based on TEM images, the diameter of undoped and boron-doped CNTs are approximately 50 nm and 40 nm, respectively. This indicates that boron-doped CNTs have smaller diameter than undoped ones. It is found that undoped CNTs have a bamboo-like shape. This shape has been reported in many studies where the Fe catalyst has been used [6–8]. Once increasing the concentration of B(OCH₃)₃ to 2 sccm, the bamboo structure disappears. In addition, Fig. 3b also shows large amount of amorphous carbon on the CNTs. SIMS results not shown here also verify the existence of boron in the nanotubes.

3.3. Raman spectroscopy

The produced CNTs were also studied by Raman spectroscopy. Raman measurements were performed using a 532-nm Ar laser with 1 cm⁻¹ resolution; integration times were 1 min at 30 mW laser power. Fig. 4 shows the Raman spectrum of undoped and

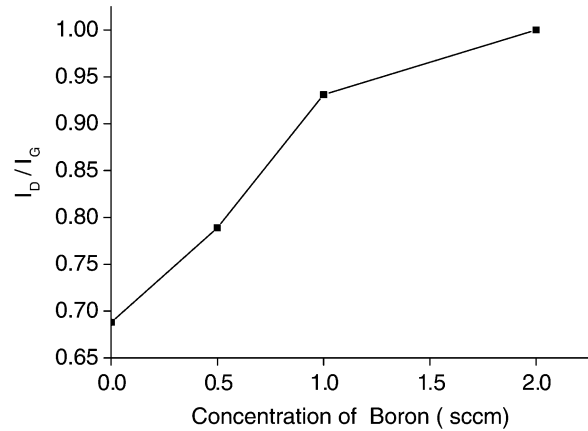


Fig. 5. I_D/I_G ratio of undoped and various concentrations of boron-doped CNTs.

boron-doped CNTs. All of them have two sharp peaks located at approximately 1350 cm⁻¹ and 1580 cm⁻¹, respectively. The first-order Raman spectrum of CNTs shows strong sharp peaks at 1581 cm⁻¹ (G line), which is the high-frequency E_{2g} first-order mode and 1350 cm⁻¹ (roughly corresponding to the D line associated with disorder-allowed zone-edge modes of graphite). The 1350 cm⁻¹ band is normally explained by relaxation of the wave vector selection rule due to the effect of the finite size of the crystal in the material [9,10]. The other conspicuous phenomenon is that the intensity of D line increases with the increasing concentration of

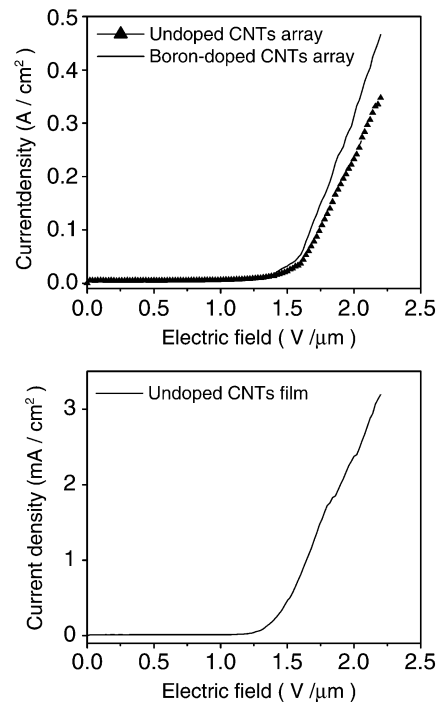


Fig. 6. Current density (*J*)–electric field (*E*) curve of undoped CNTs films, undoped and boron-doped CNTs arrays.

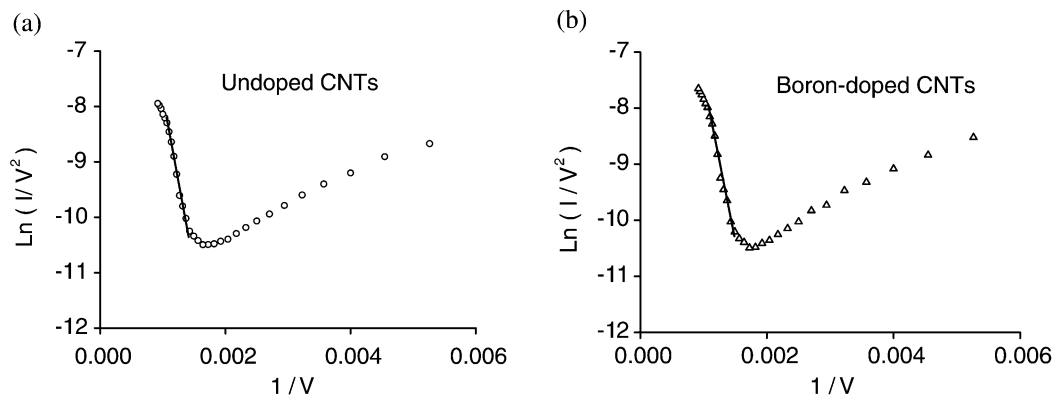


Fig. 7. F–N plot of (a) undoped and (b) boron-doped CNTs arrays.

boron. Normally, the I_D/I_G ratio increases with (i) increasing the amount of amorphous carbon in the material and (ii) decreasing the graphite crystal size. Fig. 5 indicates the I_D/I_G ratio increases with increasing the boron concentration. This implies that doping boron decreases the graphitization. Thus, the boron-doping effect strongly influences the crystallinity of CNTs. This result is also consistent with the previous TEM images.

3.4. I – V measurement

The field emission tests are performed on a diode structure, in which the CNTs are separated from the 25 cm^2 indium-tin-oxide anode using 500 μm glass spacers. The anode current is measured as a function of anode-to-cathode voltage in a vacuum of 10^{-6} Torr. The voltage is applied from 0 to 1100 V in steps at 10 V by using the Keithley SMU 237 system. Fig. 6 presents the current density vs. electric field plots for undoped and boron-doped CNTs array as well as undoped CNTs film grown in the same manner without patterning the catalyst layer. Obviously, the emitted current density for undoped CNTs array (350 mA/cm^2 at 2.2 $\text{V}/\mu\text{m}$) is much higher than for undoped CNT films (3.2 mA/cm^2 at 2.2 $\text{V}/\mu\text{m}$). This is a result of the screening effect [11,12] provoked by the proximity of neighboring CNTs. Besides, boron-doping also improves the field emission characteristics of CNT arrays by a 35% increase in the emitted current density from 350 to 470 mA/cm^2 at 2.2 $\text{V}/\mu\text{m}$. The respective Fowler–Nordheim (FN) plot ($\ln(I/V^2)$ vs. $1/V$) are shown in Fig. 7. Plotting $\ln(I/V^2)$ vs. $1/V$ results in a straight line for applied voltage higher than 700 V, implying the field emission characteristics of CNTs.

4. Conclusion

In this article, we synthesized boron-doped CNTs by using trimethylborate $\text{B}(\text{OCH}_3)_3$ as doping source. Experimental results show that undoped CNTs possess higher growth rate than boron-doped ones. In addition, the nanostructure of bamboo-like shape disappears in boron-doped CNTs. The I_D/I_G ratio increases with increasing concentration of boron, implying the decrease of graphitization in boron-doped CNTs. Doping boron clearly enhances the emission current density by 35% increase.

Acknowledgments

The authors would like to thank the National Science Council of the Republic of China for financially supporting this research under Contract No. NSC 91-2216-E-009-030.

References

- [1] S. Iijima, *Nature (London)* 354 (1991) 56.
- [2] Z.L. Wang, in: Z.L. Wang (Ed.), *Characterization of Nanophase Materials*, Wiley-VCH, New York, 1999, pp. 1–400.
- [3] Ph. Redlich, J. Loeffler, P.M. Ajayan, J. Bill, F. Aldinger, M. Ruhle, *Chem. Phys. Lett.* 260 (1996) 465.
- [4] C.L. Tsai, C.F. Chen, C.L. Lin, *J. Appl. Phys.* 90 (2001) 4847.
- [5] C.F. Chen, T.M. Hang, H.C. Chen, *J. Appl. Phys.* 74 (1993) 4483.
- [6] W. Xianbao, H. Wenping, L. Yunqi, L. Chenfeng, X. Yu, Z. Shuqin, et al., *Carbon* 39 (2001) 1533.
- [7] L.C. Jin, L.S. Chul, K. Hyoun-Woo, L.J. Ho, C.K. Ik, *Chem. Phys. Lett.* 359 (2002) 115.
- [8] L. De-Chang, D. Liming, H. Shaoming, W.H.M. Albert, L.W. Zhong, *Chem. Phys. Lett.* 316 (2000) 349.
- [9] F. Tuinstra, J.L. Koenig, *J. Chem. Phys.* 53 (1970) 1126.
- [10] R.J. Nemanich, S.A. Solin, *Phys. Rev. B* 20 (1979) 392.
- [11] P.G. Collins, A. Zettl, *Phys. Rev. B* 55 (1997) 9391.
- [12] O. Groning, O.M. Kuttel, C. Emmenegger, P. Groning, L. Shlapbach, *J. Vac. Sci. Technol. B* 18 (2000) 665.